

1 **Temporal progression of photosynthetic-strategy in**
2 **phytoplankton in the Ross Sea, Antarctica**

3

4 Thomas J. Ryan-Keogh^{a1}, Liza M. DeLizo^b, Walker O. Smith Jr.^b, Peter N. Sedwick^c,
5 Dennis J. McGillicuddy^d, C. Mark Moore^a and Thomas S. Bibby^a

6

7 ^aOcean and Earth Science, University of Southampton, National Oceanography
8 Centre, Southampton, European Way, Southampton, SO14 3ZH, U.K.

9 Email: c.moore@noc.soton.ac.uk

10 Email: tsb@noc.soton.ac.uk

11 ^bVirginia Institute of Marine Sciences, The College of William and Mary, Gloucester
12 Point, Virginia, 23062, U.S.

13 Email: delizo@vims.edu

14 Email: wos@vims.edu

15 ^cDepartment of Ocean, Earth and Atmospheric Sciences, Old Dominion University,
16 Norfolk, Virginia, 23529, U.S.

17 Email: psedwick@odu.edu

18 ^dApplied Ocean Physics and Engineering, Woods Hole Oceanographic Institute,
19 Woods Hole, Massachusetts, 02543, U.S.

20 Email: mcgillic@whoi.edu

21

22 Author for correspondence email: Thomas.Ryan-Keogh@uct.ac.za

23

24

¹ Present address: Southern Ocean Carbon and Climate Observatory, CSIR - Natural Resources and the Environment, 15 Lower Hope Road, Rosebank, Cape Town, 7700, South Africa

Abstract

The bioavailability of iron influences the distribution, biomass and productivity of phytoplankton in the Ross Sea, one of the most productive regions in the Southern Ocean. We mapped the spatial and temporal extent and severity of iron-limitation of the native phytoplankton assemblage using long- (>24 h) and short-term (24 h) iron-addition experiments along with physiological and molecular characterisations during a cruise to the Ross Sea in December-February 2012. Phytoplankton increased their photosynthetic efficiency in response to iron addition, suggesting proximal iron limitation throughout most of the Ross Sea during summer. Molecular and physiological data further indicate that as nitrate is removed from the surface ocean the phytoplankton community transitions to one displaying an iron-efficient photosynthetic strategy characterised by an increase in the size of photosystem II (PSII) photochemical cross section (σ_{PSII}) and a decrease in the chlorophyll-normalised PSII abundance. These results suggest that phytoplankton with the ability to reduce their photosynthetic iron requirements are selected as the growing season progresses, which may drive the well-documented progression from *Phaeocystis antarctica*- assemblages to diatom-dominated phytoplankton. Such a shift in the assemblage-level photosynthetic strategy potentially mediates further drawdown of nitrate following the development of iron deficient conditions in the Ross Sea.

46 **Keywords**

47 Iron, Phytoplankton, Photosynthetic proteins, Photosystem II, Nutrient limitation,

48 Ross Sea

49

50 **Highlights**

51

- 52 • Phytoplankton in the Ross Sea change their photosynthetic physiology over
53 the growing season to a strategy requiring less iron.
- 54 • This results in fluorescence yields per chlorophyll and PSII both increasing as
55 the growing season develops.
- 56 • This observation may help explain the well characterised seasonal progression
57 from to *Phaeocystis* spp. to diatom spp. over the growing season and also have
58 implications for the assessment of primary production from estimates of
59 chlorophyll in this region.

60

1. Introduction

The Ross Sea continental shelf is the most productive region in the Southern Ocean (Arrigo and van Dijken, 2004; Peloquin and Smith, 2007), with an annual productivity $>200 \text{ g C m}^{-2}$ (Smith et al., 2006), which may account for as much as 27% of the estimated total Southern Ocean biological CO_2 uptake (Arrigo et al., 2008). An understanding of the controls on primary productivity is therefore needed given the potential for future changes in stratification (Boyd et al., 2008; Smith et al., 2014) and nutrient inputs to this region (Mahowald and Luo, 2003; Tagliabue et al., 2008).

A persistent polynya in the southern Ross Sea greatly increases in size in the early austral spring (Arrigo and van Dijken, 2003; Reddy et al., 2007), and hosts large seasonal phytoplankton blooms, typically dominated by the colonial haptophyte *Phaeocystis antarctica* (*P. antarctica*) in spring through early summer (November – December), with an increase in abundance of diatoms in mid- to late summer (Arrigo and van Dijken, 2004; Arrigo et al., 1998; DiTullio and Smith, 1996; Goffart et al., 2000; Smith and Gordon, 1997; Smith et al., 2000). Understanding the causes and consequences of this seasonal phytoplankton progression is important, as the spatial and temporal distribution and abundance of *P. antarctica* and diatoms have significant biogeochemical consequences on, for example, the elemental composition and flux of biogenic material from the euphotic zone (Arrigo et al., 1999; DeMaster et al., 1992; Smith and Dunbar, 1998; Tagliabue and Arrigo, 2005).

Iron (Fe) and irradiance are assumed to exert the major ‘bottom-up’ controls on phytoplankton biogeography and productivity in the Ross Sea, given the incomplete macronutrient removal at the end of the growing season (Arrigo and van Dijken, 2003; Arrigo et al., 1998; Coale et al., 2003; Fitzwater et al., 2000; Sedwick et al., 2000; Sedwick et al., 2007; Smith et al., 2003; Smith et al., 2000; Tagliabue and Arrigo, 2003). Light availability may limit spring phytoplankton growth when vertical mixing is deep and daily integrated irradiance is low, this mixing will also supply dissolved iron (DFe) to the euphotic zone (McGillicuddy et al., 2015). As the growing season progresses and the water column stratifies, the flux of DFe from below is likely reduced and may therefore become a more significant factor in limiting

phytoplankton growth rates. Indeed, shipboard iron-addition experiments have repeatedly demonstrated the role of iron limitation in the Ross Sea (Bertrand et al., 2007; Coale et al., 2003; Cochlan et al., 2002; Martin et al., 1990; Olson et al., 2000; Sedwick and DiTullio, 1997; Sedwick et al., 2000), consistent with other metrics of Fe stress including high levels of flavodoxin (Maucher and DiTullio, 2003) and enhanced biological drawdown of silicate relative to nitrate (Arrigo et al., 2000; Smith et al., 2006).

Changes in phytoplankton composition from *P. antarctica* to diatom species may be linked to the co-limitation and interaction between iron and light. Boyd (2002) speculated that *P. antarctica* growth is limited by Fe availability from spring through late summer. Sedwick et al. (2007) further proposed that decreases in iron availability through spring are mitigated by increases in irradiance, thereby decreasing phytoplankton iron requirements. The differences in intracellular iron requirements alongside changes in the light environment may explain the community succession of the Ross Sea, where diatoms can outcompete *P. antarctica* in the late summer (Strzepek et al., 2012).

Phytoplankton that dominate in the Ross Sea may therefore need to be adapted to highly variable iron concentrations and light availability (Sedwick et al., 2011). An antagonistic relationship between irradiance and photosynthetic Fe demand may be predicted given that lower irradiances can increase Fe requirements associated with the synthesis of the additional photosynthetic units required to increase light absorption (Maldonado et al., 1999; Raven, 1990; Sunda and Huntsman, 1997). Each photosynthetic electron transfer chain requires 22-23 Fe atoms, and the photosynthetic apparatus can be the largest sink of Fe within a phytoplankton cell (Raven, 1990; Shi et al., 2007; Strzepek and Harrison, 2004). In contrast to the tight link between cellular Fe requirements and light harvesting capacity, studies on Southern Ocean diatoms and *P. antarctica* in culture suggest the Fe burden of photosynthesis may be significantly reduced for these species through increases in the size rather than the number of photosynthetic units (termed sigma-type acclimation) in response to iron/ and light limitation (Strzepek et al., 2012; Strzepek et al., 2011). Effectively, these Southern Ocean taxa appear to invest relatively more resources in the generation of a larger light-harvesting apparatus, rather than in the Fe-rich photosynthetic catalysts of photosystems I and II (Strzepek et al., 2012). This Fe-efficient strategy appears to be most pronounced for Southern Ocean diatoms, which, in culture can have some of the

largest light harvesting antennae reported (Strzepek et al., 2012), a phenotype which is more commonly associated with small cells (Suggett et al., 2009). The photosynthetic strategy of Southern Ocean diatoms may therefore contribute to the apparently low Fe requirement and cellular Fe:C ratio of these species (Coale et al., 2003; Kustka et al., 2015; Sedwick et al., 2007; Strzepek et al., 2012; Strzepek et al., 2011), and as such drive the seasonal progression from *P. antarctica* to diatoms in the Ross Sea.

In December-February 2012 a research cruise was conducted as part of the multidisciplinary research project *Processes Regulating Iron Supply at the Mesoscale – Ross Sea* (PRISM-RS), in an effort to identify and quantify the major sources of iron to the surface waters of the Ross Sea during the growing season. As part of this study, physiological and molecular measurements were combined with shipboard incubation experiments in an effort to define the spatial and temporal extent of phytoplankton iron limitation and reveal the photosynthetic strategy of the phytoplankton assemblages.

2. Materials and Methods

2.1. Oceanographic Sampling

The samples and data presented here were obtained during a cruise of the *RVIB Nathaniel B. Palmer* to the Ross Sea (cruise NBP12-01) from 24th December 2011 to 10th February 2012 (DOY 358 – 041). During the cruise, 29 short-term (24 h) and 3 long-term (168 h) incubation experiments were performed (Figure 1a). Short-term experiments were used to determine rapid iron induced changes in the phytoplankton photophysiological status; whereas long-term experiments determined whether relief from iron limitation could drive changes in biomass. For the long-term incubation experiments, uncontaminated whole seawater was collected from ~5 m depth whilst slowly underway, using a trace-metal clean towed fish system (Sedwick et al., 2011). Uncontaminated whole seawater for the short-term incubation experiments was collected from ~10 m depth in Teflon-lined, external closure 5 L Niskin-X samplers (General Oceanics) deployed on a trace metal clean CTD rosette system (Marsay et al., 2014). Samples for additional analysis were also collected along the cruise track.

2.2. Bioassay Incubation Experiments

Incubation experiments were performed using methods similar to those employed previously in the Southern Ocean (Moore et al., 2007; Nielsdóttir et al., 2012) and the high latitude North Atlantic (HLNA) (Nielsdóttir et al., 2009; Ryan-Keogh et al., 2013). Water for the experiments (see 2.1, above) was transferred unscreened into acid-washed 1.0-L polycarbonate bottles (Nalgene) for the short-term incubation experiments and 4.5-L polycarbonate bottles for the long-term incubation experiments. Incubation bottles were filled in a random order, with triplicate samples for initial measurements in the long-term incubation experiments collected at the beginning, middle and end of the filling process. Initial samples for the short-term incubation experiments were collected from the same Niskin-X sampling bottle. The short-term experiments were run for 24 h and the long-term experiments were run for 168 h; both experiments consisted of two treatments: an unamended control treatment

and 2.0 nmol L⁻¹ Fe treatment (hereafter, + Fe). All experimental incubations were conducted as biological duplicates or triplicates.

All bottle tops were externally sealed with film (ParafilmTM), and bottles were double bagged with clear polyethylene bags to minimize risks of contamination during the incubation. On-deck incubators were shaded using LEE “blue lagoon” filters to provide light levels corresponding to ~35% of above-surface irradiance (Hinz et al., 2012; Nielsdóttir et al., 2009; Ryan-Keogh et al., 2013). Flowing surface seawater was used to control the temperature in the incubators. Subsampling of long-term incubations for measurements of chlorophyll *a*, dissolved macronutrient concentrations and phytoplankton physiological parameters occurred after 24, 72, 120 and 168 h. Sub-sampling of short-term incubation experiments for the same parameters occurred after 24 h. All experiments were set up and sub-sampled under a class-100 laminar flow hood within a trace metal clean environment.

2.3. Chlorophyll *a* and Nutrient Analysis

Samples for chlorophyll *a* (Chl) analysis (250 mL) were filtered onto GF/F filters and then extracted into 90% acetone for 24 h in the dark at 4°C, followed by analysis with a fluorometer (TD70; Turner Designs) (Welschmeyer, 1994). Macronutrient samples were drawn into 50 mL diluvials and refrigerated at 4°C until analysis, which typically commenced within 12 h of sampling. Nitrate plus nitrite (DIN), phosphate, ammonium and silicate were determined shipboard on a five-channel Lachat Instruments QuikChem FIA+ 8000s series AutoAnalyser (Armstrong et al., 1967; Atlas et al., 1971; Bernhardt and Wilhelms, 1967; Patton, 1983). Dissolved iron was determined post-cruise using flow injection analysis modified from Measures et al. (1995), as described by Sedwick et al. (2011); accuracy of the DFe method was verified by analysis of SAFe reference seawater samples (Johnson et al., 2007).

2.4. Phytoplankton Photosynthetic Physiology

Variable chlorophyll fluorescence was measured using a Chelsea Scientific Instruments FastrackaTM Mk II Fast Repetition Rate fluorometer (FRRf) integrated with a FastActTM Laboratory system. All samples were acclimated in opaque bottles for 30 minutes at *in situ* temperatures, and FRRf measurements were blank corrected

effect using carefully prepared 0.2 μm filtrates for all samples (Cullen and Davis, 2003). Blanks were typically around 1% and always <10% of the maximum fluorescence signal. Protocols for FRRf measurements and data processing were similar to those detailed elsewhere (Moore et al., 2007). Data from the FRRf were analysed to derive values of the minimum and maximum fluorescence (F_o and F_m) and hence F_v/F_m (where $F_v = F_m - F_o$), as well as the functional absorption cross-section of PSII (σ_{PSII}) by fitting transients to the model of Kolber et al. (1998).

2.5. Phytoplankton Composition

Samples for photosynthetic pigment analysis were collected and measured by high performance liquid chromatography (HPLC). 0.3 – 1.0 L of sea-water were filtered through GF/F filters, which were immediately flash frozen in liquid nitrogen and stored at -80°C until analysis. Pigments were extracted into 90% acetone by sonification before quantification using a Waters Spherisorb ODSU C-18 HPLC column and Waters HPLC system as described in Smith et al. (2006). Algal community composition was then estimated from pigment concentrations following the method of Arrigo et al. (1999).

2.6. Total Protein Extraction and Quantification

Photosynthetic protein abundances were quantified using techniques similar to those described elsewhere (Brown et al., 2008; Macey et al., 2014; Ryan-Keogh et al., 2012). Samples for protein extraction were collected by filtering 1.0-3.0 L of seawater onto GF/F filters (Whatman) under low light for ~45 minutes to minimize changes in protein abundance following sampling. Filters were flash frozen and stored at -80°C until analysis. Proteins were extracted in the laboratory according to the protocol described by Brown et al. (2008). Quantification was performed using custom Agrisera™ primary antibodies and peptide standards, which were designed against peptide tags conserved across all oxygenic photosynthetic species for protein subunits that are representative of the functional photosynthetic complex PsbA (PSII) (Campbell et al., 2003). Protein abundances were quantified using QuantityOne™ and ImageLab™ software; quantification was performed within the unsaturated portion of the calibration curve. The estimated protein abundances were comparable to those

243 reported for natural phytoplankton communities using similar methods (Hopkinson et
244 al., 2010; Losh et al., 2013; Macey et al., 2014; Richier et al., 2012).
245

3. Results and Discussion

3.1. General Oceanography

A range of oceanographically distinct regions was occupied on the Ross Sea continental shelf during the PRISM-RS cruise (Figure 1). These included areas close to the Ross Ice Shelf, near and within pack ice, and over shallow bathymetric features, both of which may provide important sources of DFe to the upper water column (McGillicuddy et al., 2015). Highest chlorophyll *a* concentrations (Figure 2a) were associated with the ice-shelf in the southwestern Ross Sea ($24.6 \mu\text{g Chl L}^{-1}$) and correlated with the lowest DIN (dissolved inorganic nitrate + nitrite) concentrations (Figure 2b, Figure 3) and lowest surface F_v/F_m values observed (Figure 2c, Figure 3). Surface DFe concentrations ranged from 0.067-0.787 nM (Figure 2d), were not correlated with chlorophyll or DIN concentrations (Figure 3, Supplementary Information, Figure S1), and were elevated off the continental shelf in the northeast sector of the Ross Sea.

3.2. Mapping of Iron Limitation

Despite being the most productive region in the Southern Ocean, our results confirm that phytoplankton growth in the Ross Sea is limited by iron availability during summer, consistent with previous studies (Bertrand et al., 2011; Bertrand et al., 2007; Coale et al., 2003; Cochlan et al., 2002; Martin et al., 1990; Olson et al., 2000; Sedwick and DiTullio, 1997; Sedwick et al., 2000). The response of phytoplankton to iron-addition was assayed through a series of long- (168 h) and short-term (24 h) iron-addition incubations (Figure 1), while no clear spatial pattern in iron stress could be observed from a single cruise during a time of relatively rapid changes in a spatio-temporally complex system (Figure 2), there was evidence of an increase in photosynthetic efficiency following iron addition throughout much of the Ross Sea during summer, highlighting the role of iron in influencing phytoplankton physiology. To compare these iron-mediated changes in F_v/F_m , $\Delta(F_v/F_m)$ was calculated as defined in Ryan-Keogh et al. (2013), as the difference between the Fe-amended and control treatments (Equation 1).

Equation 1 Calculation of $\Delta(F_v/F_m)$.

$$\Delta(F_v/F_m) = \frac{F_v/F_{m+Fe} - F_v/F_{m_{Control}}}{Time}$$

Values of $\Delta(F_v/F_m)$ were frequently positive following iron addition (ranging from 0.00 - 0.17) (Figure 4a), suggesting that Fe amendments increased the photosynthetic efficiency of phytoplankton in much of the Ross Sea during the sampling period.

Data from long-term (168 h) experiments (Table 1 and Figure 4) enable a more detailed analysis of the response of phytoplankton to iron-additions. Three experiments were initiated from (1) near the Ross Ice Shelf, (2) over the Ross Bank and (3) in an anti-cyclonic eddy (Figure 1 and Figure 4). The three experiments revealed varying responses to iron additions by the extant phytoplankton assemblage. Experiments 1 and 3 gave a strong and positive response to iron additions, and provided evidence that phytoplankton were iron limited. Shorter-term responses revealed elevated values of F_v/F_m (i.e., a positive $\Delta(F_v/F_m)$) after 24 h (Figure 4a), with subsequent significant (ANOVA, $p<0.05$) increases in growth rates and nutrient removal observed after 168 h (Table 1). Experiment 2, initiated over the Ross Bank, did not show an increase in photosynthetic efficiency $\Delta(F_v/F_m)$ (Figure 4a). Moreover, growth rate and nutrient removal were not significantly different between control and iron-addition conditions until after >168 h (ANOVA, $p>0.05$) (Table 1), which most likely reflects severe depletion of ambient DFe in the control treatments by this time. The Ross Bank (Figure 4a, Table 1) has a shallow bathymetry (~150 m), and none of the Fe-addition experiments in this region showed a significant response (Figure 4). The Ross Bank may therefore provide significant and continuous DFe inputs to the euphotic zone, thereby ultimately stimulating productivity.

The measurement of F_v/F_m is derived from analysis of the fluorescence kinetics emitted from the photosynthetic reaction centre photosystem II (PSII) and its associated light-harvesting antenna (Kolber and Falkowski, 1993). Understanding the mechanism of changes to F_v/F_m can provide information on the process by which phytoplankton respond to iron-limitation. Absolute changes in maximum fluorescence (F_m) and variable fluorescence (F_v) normalised to chlorophyll *a* were calculated (Figure 4b and 4c), revealing a significant difference between the +Fe and control treatments in $F_m \text{ Chl}^{-1}$ ($t = 24 \text{ h}$ (t -test, $p<0.05$)), whereas there was no significant difference for $F_v \text{ Chl}^{-1}$ ($t = 24 \text{ h}$ (t -test, $p>0.05$)). This suggests that changes in F_v/F_m

reflect changes in the proportion of chlorophyll that is photosynthetically coupled to active PSII reaction centres, rather than changes in the activity of PSII (Behrenfeld et al., 2006; Lin et al., 2016; Macey et al., 2014). A similar response was observed for all short-term iron-addition experiments that exhibited positive changes in $\Delta(F_v/F_m)$.

3.3 Temporal Development of Photosynthetic Strategy

Given the high degree of spatial variability in response to iron-additions, we placed all observations within a unified framework, hence producing a conceptualised model of temporal progression of phytoplankton within the Ross Sea. The PRISM-RS cruise sampled for 30 days covering a period from mid- to late summer, during which we expected iron limitation of phytoplankton growth to be significant (Sedwick et al., 2000). Total phytoplankton biomass accumulation is dependent on growth after the sampled regions become ice-free (Arrigo and van Dijken, 2003) and the losses due to grazing, sinking and physical removal. All spatial data therefore represent a mosaic of different temporal progressions that represent different stages of phytoplankton development. We utilise surface nitrate (DIN) as a proxy to separate the temporal patterns from any spatial differences (Figure 5). As phytoplankton biomass (Chl) increased, nutrients were removed and F_v/F_m reduced (Figure 3, Figure 5a). Pigment data showed that the nutrient drawdown and Chl increase in parallel with a shift from *P. antarctica*-dominated to diatom-dominated assemblages (Figure 3, Figure 5b). Within this conceptual framework, the relative severity of Fe-stress ($\Delta F_v/F_m$) may be inferred from the Fe-addition incubation experiments. Two potential phases of Fe deficiency were identified (Figure 5c): first, when DIN concentrations remain high ($> \sim 20 \mu\text{M}$) and *P. antarctica* is a major component of the phytoplankton (labelled '1'), and secondly when DIN is further removed (to $< \sim 20 \mu\text{M}$) by diatom-dominated communities (labelled '2'; Figure 5c).

Photophysiological parameters are presented within this framework. The relative size of the effective light-harvesting cross-section of PSII (σ_{PSII}) (Figure 6a) is low ($\sim 1.6 \text{ nm}^{-2}$) when DIN and F_v/F_m are high, and approximately doubles to $\sim 3.29 \text{ nm}^{-2}$ as DIN is depleted and the assemblage becomes diatom-dominated. Quantification of the photosynthetic catalyst PSII further characterises the photosynthetic strategy of phytoplankton in the Ross Sea. Chlorophyll normalised to abundances of the protein target PsbA (indicative of the abundance of PSII; (Brown et

al., 2008) (Chl:PsbA), which can provide another indication of the relative sizes of the light harvesting pigment antenna relative the abundance of the photosystems, is lower at higher DIN concentrations and increases as DIN and F_v/F_m decrease (Figure 6b). Combining the protein abundance data and the photophysiological measurements, the maximum fluorescent yield per chlorophyll (F_m :Chl) (Figure 6c) and per PSII (F_m :PsbA) (Figure 6d) can also be calculated. Both of these parameters increase, by 46 and 296% respectively, with decreases in DIN and F_v/F_m .

Together, these photophysiological measurements and corresponding environmental information at the time of sampling therefore indicate several significant correlations (Figure 3 & Supplementary Information, S1) associated with the potential drivers of the observed transition in community structure and subsequent changes in photophysiology. Thus, within our conceptual frame work, using DIN concentration as a proxy for the stage of the phytoplankton bloom, we observe statistically significant positive correlations ($p<0.01$) with other macronutrients and the photosynthetic efficiency (F_v/F_m) which all decline as nitrate is removed from the system. While negative correlations ($p<0.01$) are observed between DIN and temperature, chlorophyll concentration, the relative abundance of diatoms and σ PSII which all increase as nitrate is removed from the system. While no significant correlation is seen between DIN and the fluorescence yield per PSII (F_m :PSII) or the chlorophyll content per PSII (Chl:PSII), there is a significant negative correlation between F_m :Chl and PSII:Chl ($p<0.01$) (Figure 3).

No statistically significant ($p<0.01$) relationships were observed with dissolved iron concentrations, suggesting that this variable may not represent a good indicator of iron stress, as might be expected considering that any limiting nutrient would be expected to be severely depleted by biological uptake. Overall, the observed correlations are thus taken to be indicative of the phytoplankton community transitioning between dominant groups as SST increases, non-limiting macronutrients are drawn down and the community biomass increases, potential as a result of different Fe utilisation capacities between diatoms and *P. antarctica* (Strzepek et al., 2012). These observations may also support that the hypothesis that Southern Ocean diatoms may both acquire (Kustka et al., 2015) and utilise (Strzepek et al., 2012) iron more effectively than *P. antarctica* and that the community transition may enable further drawdown of nitrate.

While there can be an array of reasons for diatoms being better at acquiring and utilising available DFe as it becomes limiting during summer in the Ross Sea, differences in photosynthetic strategy have the potential to be a significant factor in regulating the temporal changes that occur, given that the photosynthetic apparatus represents the dominant sink for Fe in a phytoplankton cell (Raven, 1990; Strzepek and Harrison, 2004). The analysis presented here clearly demonstrates that a different photosynthetic strategy is apparent within the phytoplankton community responsible for the initial DIN removal vs. those responsible for the later DIN removal. These observations of photosynthetic strategy are consistent with some of the ecophysiological differences observed within culture-based studies of Southern Ocean phytoplankton (Strzepek et al., 2012). Phytoplankton in the Ross Sea generally display a large, functional light-harvesting cross section for PSII (σ_{PSII}) compared to temperate species (Smith et al., 2011). As has been proposed (Strzepek et al., 2012), this may reflect a strategy by which cells acclimate and/or adapt through increasing the size of photosynthetic units rather than the number of photosynthetic units in a low Fe environment – thus escaping the typical antagonistic relationship between iron-demand and light capture (Sunda and Huntsman, 1997). Our measurements of the abundance of the photosynthetic catalysis PSII were also consistent with such an observation, whereby the increase in the ratio of Chl:PSII mirrors the increase in σ_{PSII} (Figure 6b). This strategy could significantly reduce the iron-demand normally associated with the photosynthetic apparatus. Phytoplankton that dominate at low DIN have a particularly large σ_{PSII} and have increased Chl:PSII values by 255%, again in agreement with culture studies in which Southern Ocean diatoms have larger σ_{PSII} than *P. antarctica* (Strzepek et al., 2012).

We thus suggest that the diatoms that dominate in summer as DIN is removed may represent a refined strategy to reduced iron availability, noting that previous information from temperate taxa and regions (Suggett et al., 2009) would tend to suggest that relatively high functional cross sections would be unlikely in phytoplankton with large cell sizes typical of many Southern Ocean diatoms (Suggett et al., 2009). Large cells with large σ_{PSII} may, however, result in ecophysiological trade-offs, including a tendency for over-excitation of PSII and photodamage, which may require a rapid PSII repair cycle or a requirement for rapidly inducible and significant non-photochemical quenching (Campbell and Tyystjärvi, 2012; Petrou et al., 2010; Wu et al., 2011), possibly suggesting Antarctic diatoms would require novel

photoprotective strategies. Despite these potential negative consequences of a large σ_{PSII} , Antarctic diatoms seem to have adopted a phenotypic response underlining the relevance of iron-availability and providing some explanation for the low Fe:C ratios in some of these species (Strzepek et al., 2012).

While the observations in this study were restricted to the summer season they do include DIN concentrations similar to those estimated for the winter mixed layer nitrate concentration (McGillicuddy et al., 2015) and so potentially conditions analogous to a broader seasonal progression in phytoplankton composition in the Ross Sea from *P. antarctica* early in the growing season to diatom-dominance later in summer (Smith et al., 2010). The dataset therefore provides indications of potential contributory mechanisms for this seasonal progression, while also reflecting the large degree of spatial heterogeneity in physical and biological processes throughout the growing season in the Ross Sea (Smith and Jones, 2015).

The data presented here also provide insights into the mechanism of the iron-stress response of phytoplankton. Increases in F_v/F_m are commonly reported as a response to Fe addition (Boyd et al., 2008; Feng et al., 2010). Results from the experiments and observations show that increases in F_v/F_m in response to Fe addition and elevated F_v/F_m values in regions with modest DIN drawdown result from reduction in the ratio of $F_m:\text{Chl}$ (or $F_m:\text{PSII}$) rather than changes in $F_v:\text{Chl}$. This is in agreement with similar observations from the high latitude North Atlantic and Equatorial Pacific (Behrenfeld et al., 2006; Lin et al., 2016; Macey et al., 2014) regions and implies that low F_v/F_m results from changes in the coupling of light-harvesting chlorophyll-binding proteins to photosynthesis rather than accumulation of damaged photosystems. Such accumulation of non-photosynthetically active chlorophyll-binding proteins in Fe-limited oceanic regions can have consequences on estimates of productivity in these regions (Behrenfeld et al., 2006).

4. Conclusions

The current study represents an analysis of the summer photosynthetic strategies of phytoplankton in the Ross Sea and highlights how different iron-efficiency strategies occur in phytoplankton as Fe becomes limiting and irradiance availability becomes maximal. This is important for understanding Fe usage efficiency in the region. The Ross Sea clearly differs from other high latitude regions due to plankton composition, yet iron availability still contributes to reduced growth rates and macronutrient removal. Even though this system is one of the most productive regions in the Southern Ocean, iron availability still exerts a strong control over summer productivity and biomass accumulation, and any changes in future iron supply induced by climate change could have profound effects. Climate-mediated changes to the mixed layer depth and sea-ice cover could change iron limitation strategies and phytoplankton phenology (Boyd et al., 2012), as well as alterations to iron supply from highly variable supply mechanisms such as Australian and local dust inputs (Mackie et al., 2008). The Southern Ocean is predicted to be particularly biogeochemically significant with respect to climate change (Marinov et al., 2006) and is the only iron-limited HNLC region where the cryosphere plays a major role. An understanding of the role of iron limitation in this highly dynamic environment is thus particularly important; particularly as climate mediated variability is expected to increase.

Acknowledgements

We thank the captain and crew of the RVIB *Nathaniel B. Palmer* during research cruise NBP12-01, alongside all the scientists involved in the cruise. Chris Marsay performed the DFe determinations. This research was supported by grants from the National Science Foundation (ANT-0944254 to W.O.S., ANT-0944174 to P.N.S.), and a NERC PhD studentship to TRK.

5. References

- Armstrong, F.A.J., Stearns, C.R., Strickland, J.D.H., 1967. The measurement of upwelling and subsequent biological processes by means of the Technicon AutoAnalyzer and associate equipment. *Deep-Sea Research* 14, 381-389.
- Arrigo, K.R., DiTullio, G.R., Dunbar, R.B., Robinson, D.H., VanWoert, M., Worthen, D.L., Lizotte, M.P., 2000. Phytoplankton taxonomic variability in nutrient utilization and primary production in the Ross Sea. *J Geophys Res* 105, 8827-8845.
- Arrigo, K.R., Robinson, D.H., Worthen, D.L., Dunbar, R.B., DiTullio, G.R., VanWoert, M., Lizotte, M.P., 1999. Phytoplankton community structure and the drawdown of nutrients and CO₂ in the Southern Ocean. *Science* 283, 365-367.
- Arrigo, K.R., van Dijken, G.L., 2003. Phytoplankton dynamics within 37 Antarctic coastal polynya systems. *J Geophys Res* 108, 3271.
- Arrigo, K.R., van Dijken, G.L., 2004. Annual changes in sea-ice, chlorophyll a, and primary production in the Ross Sea, Antarctica. *Deep-Sea Research II* 51, 117-138.
- Arrigo, K.R., van Dijken, G.L., Long, M., 2008. Coastal Southern Ocean: A strong anthropogenic CO₂ sink. *Geophysical Research Letters* 35, L21602.
- Arrigo, K.R., Worthen, D., Schnell, A., Lizotte, M.P., 1998. Primary production in Southern Ocean waters. *J Geophys Res* 103, 15587-15600.
- Atlas, e.l., Hager, S.W., Gordon, L.I., Park, P.K., 1971. A practical manual for use of the Technicon Autoanalyzer in seawater nutrient analyses: revised, Technical Report 215. Oregon State University, p. 48.
- Behrenfeld, M.J., Worthington, K., Sherrell, R.M., Chavez, F.P., Strutton, P., McPhaden, M., Shea, D.M., 2006. Controls on tropical Pacific Ocean productivity revealed through nutrient stress diagnostics. *Nature* 442, 1025-1028.
- Bernhardt, H., Wilhelms, A., 1967. The continuous determination of low level iron, soluble phosphate and total phosphate with the AutoAnalyzer, Technicon Symposium, p. 386.
- Bertrand, E.M., Saito, M.A., Lee, P.A., Dunbar, R.B., Sedwick, P.N., DiTullio, G.R., 2011. Iron limitation of a springtime bacterial and phytoplankton community in the Ross Sea: implications for vitamin b(12) nutrition. *Frontiers in microbiology* 2, 160.

497 Bertrand, E.M., Saito, M.A., Rose, J.M., Riesselman, C.R., Lohan, M.C., Noble, A.E.,
 498 Lee Peter, A., DiTullio, G.R., 2007. Vitamin B12 and iron co-limitation of
 499 phytoplankton growth in the Ross Sea. *Limnol Oceanogr* 52, 1078-1093.
 500 Boyd, P.W., 2002. Environmental factors controlling phytoplankton processes in the
 501 Southern Ocean. *J Phycol* 38, 844-861.
 502 Boyd, P.W., Arrigo, K.R., Strzepek, R., van Dijken, G.L., 2012. Mapping
 503 phytoplankton iron utilization: Insights into Southern Ocean supply mechanisms. *J*
 504 *Geophys Res* 117, C06009.
 505 Boyd, P.W., Doney, S.C., Strzepek, R., Dusenberry, J., Lindsay, K., Fung, I., 2008.
 506 Climate-mediated changes to mixed-layer properties in the Southern Ocean: assessing
 507 the phytoplankton response. *Biogeosciences* 5, 847-864.
 508 Brown, C.M., MacKinnon, J.D., Cockshutt, A.M., Villareal, T.A., Campbell, D.A.,
 509 2008. Flux capacities and acclimation costs in *Trichodesmium* from the Gulf of
 510 Mexico. *Marine Biology* 154, 413-422.
 511 Campbell, D.A., Cockshutt, A.M., Porankiewicz-Asplund, J., 2003. Analysing
 512 photosynthetic complexes in uncharacterized species or mixed microalgal communities
 513 using global antibodies. *Physiol Plant* 119, 322-327.
 514 Campbell, D.A., Tyystjärvi, E., 2012. Parameterization of photosystem II
 515 photoinactivation and repair. *Biochim Biophys Acta* 1817, 258-265.
 516 Coale, K.H., Wang, X.J., Tanner, S.J., Johnson, K.S., 2003. Phytoplankton growth
 517 and biological response to iron and zinc addition in the Ross Sea and Antarctic
 518 Circumpolar Current along 170 degrees W. *Deep-Sea Research II* 50, 635-653.
 519 Cochlan, W.P., Bronk, D.A., Coale, K.H., 2002. Trace metals and nitrogenous
 520 nutrition of Antarctic phytoplankton: experimental observations in the Ross Sea.
 521 *Deep-Sea Research II* 49, 3365-3390.
 522 Cullen, J.J., Davis, R.F., 2003. The blank can make a big difference in oceanographic
 523 measurements. *Limnology and Oceanography Bulletin* 12, 29-35.
 524 DeMaster, D.J., Dunbar, R.B., Gordon, L.I., Leventer, A.R., Morrison, J.M., Nelson,
 525 D.M., Nittrouer, C.A., Smith, W.O., Jr., 1992. Cycling and accumulation of biogenic
 526 silica and organic matter in high-latitude environments: The Ross Sea. *Oceanography*
 527 5, 146-153.
 528 DiTullio, G.R., Smith, W.O., 1996. Spatial patterns in phytoplankton biomass and
 529 pigment distributions in the Ross Sea. *J Geophys Res* 101, 18467-18477.

530 Feng, Y., Hare, C.E., Rose, J.M., Handy, S.M., DiTullio, G.R., Lee, P.A., Smith,
 531 W.O., Jr., Peloquin, J., Tozzi, S., Sun, J., Zhang, Y., Dunbar, R.B., Long, M.C.,
 532 Sohst, B., Lohan, M., Hutchins, D.A., 2010. Interactive effects of iron, irradiance and
 533 CO₂ on Ross Sea phytoplankton. *Deep-Sea Research I* 57, 368-383.
 534 Fitzwater, S.E., Johnson, K.S., Gordon, R.M., Coale, K.H., Smith, W.O., Jr., 2000.
 535 Trace metal concentrations in the Ross Sea and their relationship with nutrients and
 536 phytoplankton growth. *Deep-Sea Research II* 47, 3159-3179.
 537 Goffart, A., Catalano, G., Hecq, J.H., 2000. Factors controlling the distribution of
 538 diatoms and *Phaeocystis* in the Ross Sea. *Journal of Marine Systems* 27, 161-175.
 539 Hinz, D.J., Nielsdóttir, M.C., Korb, R.E., Whitehouse, M.J., Poulton, A.J., Moore,
 540 C.M., Achterberg, E.P., Bibby, T.S., 2012. Responses of microplankton community
 541 structure to iron addition in the Scotia Sea. *Deep-Sea Research II* 59, 36-46.
 542 Hopkinson, B.M., Xu, Y., Shi, D., McGinn, P.J., Morel, F.M.M., 2010. The effect of
 543 CO₂ on the photosynthetic physiology of phytoplankton in the Gulf of Alaska. *Limnol*
 544 *Oceanogr* 55, 2011-2024.
 545 Johnson, K.S., Elrod, V.A., Fitzwater, S.E., Plant, J., Boyle, E., Bergquist, B.,
 546 Bruland, K.W., Aguilar-Islas, A.M., Buck, K., Lohan, M.C., Smith, G.J., Sohst, B.M.,
 547 Coale, K.H., Gordon, M., Tanner, S., Measures, C.I., Moffett, J., Barbeau, K.A.,
 548 King, A., Bowie, A.R., Chase, Z., Cullen, J.J., Laan, P., Landing, W., Mendez, J.,
 549 Milne, A., Obata, H., Doi, T., Osslander, L., Sarthou, G., Sedwick, P.N., Van den
 550 Berg, S., Laglera-Baquer, L., Wu, J.-F., Cai, Y., 2007. Developing standards for
 551 dissolved iron in seawater. *Eos, Transactions American Geophysical Union* 88, 131-
 552 132.
 553 Kolber, Z.S., Falkowski, P.G., 1993. Use of active fluorescence to estimate
 554 phytoplankton photosynthesis in situ. *Limnol Oceanogr* 38, 1646-1665.
 555 Kolber, Z.S., Prášil, O., Falkowski, P.G., 1998. Measurements of variable chlorophyll
 556 fluorescence using fast repetition rate techniques: defining methodology and
 557 experimental protocols. *Biochim Biophys Acta* 1367, 88-106.
 558 Kustka, A.B., Jones, B.M., Hatta, M., Field, M.P., Milligan, A.J., 2015. The influence
 559 of iron and siderophores on eukaryotic phytoplankton growth rates and community
 560 composition in the Ross Sea. *Mar Chem* 173, 195-207.
 561 Lin, H., Kuzimov, F.I., Park, J., Lee, S., Falkowski, P.G., Gorbunov, M.Y., 2016. The
 562 fate of photons absorbed by phytoplankton in the global ocean. *Science* 351, 264-267.

563 Losh, J.L., Young, J.N., Morel, F.M.M., 2013. Rubisco is a small fraction of total
 564 protein in marine phytoplankton. *New Phytol* 198, 52-58.
 565 Macey, A.I., Ryan-Keogh, T.J., Richier, S., Moore, C.M., Bibby, T.S., 2014.
 566 Photosynthetic protein stoichiometry and photophysiology in the high latitude North
 567 Atlantic. *Limnol Oceanogr* 59, 1853-1864.
 568 Mackie, D.S., Boyd, P.W., McTainsh, G.H., Tindale, N.W., Westberry, T.K., Hunter,
 569 K.A., 2008. Biogeochemistry of iron in Australian dust: From eolian uplift to marine
 570 uptake. *Geochemistry, Geophysics, Geosystems* 9, Q03Q08.
 571 Mahowald, N.M., Luo, C., 2003. A less dusty future? *Geophysical Research Letters*
 572 30, 1903 doi:10.1029/2003GL917880.
 573 Maldonado, M.T., Boyd, P.W., Harrison, P.J., Price, N.M., 1999. Co-limitation of
 574 phytoplankton growth by light and Fe during winter in the NE subarctic Pacific
 575 Ocean. *Deep-Sea Research II* 46, 2475-2485.
 576 Marinov, I., Gnanadesikan, A., Toggweiler, J.R., Sarmiento, J.L., 2006. The Southern
 577 Ocean biogeochemical divide. *Nature* 441, 964-967.
 578 Marsay, C.M., Sedwick, P.N., Dinniman, M.S., Barrett, P.M., Mack, S.L.,
 579 McGillicuddy, D.J., 2014. Estimating the benthic efflux of dissolved iron on the Ross
 580 Sea continental shelf. *Geophysical Research Letters* 41, 7576-7583.
 581 Martin, J.H., Gordon, R.M., Fitzwater, S.E., 1990. Iron in Antarctic waters. *Nature*
 582 345, 156-158.
 583 Maucher, J.M., DiTullio, G.R., 2003. Flavodoxin as a diagnostic indicator of chronic
 584 iron limitation in the Ross Sea and New Zealand sector of the Southern Ocean,
 585 Biogeochemistry of the Ross Sea. American Geophysical Union, Washington D.C.,
 586 pp. 35-52.
 587 McGillicuddy, D.J., Sedwick, P.N., Dinniman, M.S., Arrigo, K.R., Bibby, T.S.,
 588 Greenan, B.J.W., Hofmann, E.E., Klinck, J.M., Smith, W.O., Jr., Mack, S.L., Marsay,
 589 C.M., Sohst, B.M., van Dijken, G.L., 2015. Iron supply and demand in an Antarctic
 590 shelf ecosystem. *Geophysical Research Letters*.
 591 Measures, C.I., Yuan, J., Resing, J.A., 1995. Determination of iron in seawater by
 592 flow injection analysis using in-line preconcentration and spectrophotometric
 593 detection. *Mar Chem* 50, 3-12.
 594 Moore, C.M., Seeyave, S., Hickman, A.E., Allen, J.T., Lucas, M.I., Planquette, H.,
 595 Pollard, R.T., Poulton, A.J., 2007. Iron-light interactions during the CROZet natural

596 iron bloom and EXport experiment (CROZEX) I: Phytoplankton growth and
 597 photophysiology. *Deep-Sea Research II* 54, 2045-2065.

598 Nielsdóttir, M.C., Bibby, T.S., Moore, C.M., Hinz, D.J., Sanders, R., Whitehouse, M.,
 599 Korb, R., Achterberg, E.P., 2012. Seasonal and spatial dynamics of iron availability in
 600 the Scotia Sea. *Mar Chem* 130, 62-72.

601 Nielsdóttir, M.C., Moore, C.M., Sanders, R., Hinz, D.J., Achterberg, E.P., 2009. Iron
 602 limitation of the postbloom phytoplankton communities in the Iceland Basin. *Global*
 603 *Biogeochemical Cycles* 23, 1-13.

604 Olson, R.J., Sosik, H.M., Chekalyuk, A.M., Shalapyonok, A., 2000. Effects of iron
 605 enrichment on phytoplankton in the Southern Ocean during late summer: active
 606 fluorescence and flow cytometric analyses. *Deep-Sea Research II* 47, 3181-3200.

607 Patton, C.J., 1983. Design, characterization and applications of a miniature continuous
 608 flow analysis system. Michigan State University, Ann Arbor, Michigan.

609 Peloquin, J.A., Smith, W.O., Jr., 2007. Phytoplankton blooms in the Ross Sea,
 610 Antarctica: Interannual variability in magnitude, temporal patterns, and composition. *J*
 611 *Geophys Res* 112, C08013.

612 Petrou, K., Hill, R., Brown, C.M., Campbell, D.A., Doblin, M.A., Ralph, P.J., 2010.
 613 Rapid photoprotection in sea-ice diatoms from the East Antarctic pack ice. *Limnol*
 614 *Oceanogr* 55, 1400-1407.

615 Raven, J.A., 1990. Predictions of Mn and Fe use efficiencies of phototrophic growth
 616 as a function of light availability for growth and C assimilation pathway. *New Phytol*
 617 116, 1-18.

618 Reddy, T.E., Arrigo, K.R., Holland, D.M., 2007. The role of thermal and mechanical
 619 processes in the formation of the Ross Sea summer polynya. *J Geophys Res* 112.

620 Richier, S., Macey, A.I., Pratt, N.J., Honey, D.J., Moore, C.M., Bibby, T.S., 2012.
 621 Abundances of Iron-Binding Photosynthetic and Nitrogen-Fixing Proteins of
 622 *Trichodesmium* Both in Culture and In Situ from the North Atlantic. *Plos One* 7,
 623 e35571.

624 Ryan-Keogh, T.J., Macey, A.I., Cockshutt, A.M., Moore, C.M., Bibby, T.S., 2012.
 625 The cyanobacterial chlorophyll-binding-protein IsiA acts to increase the *in vivo*
 626 effective absorption cross-section of photosystem I under iron limitation. *J Phycol* 48,
 627 145-154.

628 Ryan-Keogh, T.J., Macey, A.I., Nielsdóttir, M., Lucas, M.I., Steigenberger, S.S.,
 629 Stinchcombe, M.C., Achterberg, E.P., Bibby, T.S., Moore, C.M., 2013. Spatial and

630 temporal development of phytoplankton iron stress in relation to bloom dynamics in
631 the high-latitude North Atlantic Ocean. *Limnol Oceanogr* 58, 533-545.

632 Sedwick, P.N., DiTullio, G.R., 1997. Regulation of algal blooms in Antarctic shelf
633 waters by the release of iron from melting sea ice. *Geophysical Research Letters* 24,
634 2515-2518.

635 Sedwick, P.N., DiTullio, G.R., Mackey, D.J., 2000. Iron and manganese in the Ross
636 Sea, Antarctica: seasonal iron limitation in Antarctic shelf waters. *J Geophys Res* 105,
637 11321-11336.

638 Sedwick, P.N., Garcia, N.S., Riseman, S.F., Marsay, C.M., DiTullio, G.R., 2007.
639 Evidence for high iron requirements of colonial *Phaeocystis antarctica* at low
640 irradiance. *Biogeochemistry* 83, 83-97.

641 Sedwick, P.N., Marsay, C.M., Sohst, B.M., Aguilar-Islas, A.M., Lohan, M.C., Long,
642 M.C., Arrigo, K.R., Dunbar, R.B., Saito, M.A., Smith, W.O., Jr., DiTullio, G.R.,
643 2011. Early season depletion of dissolved iron in the Ross Sea polynya: implications
644 for iron dynamics on the Antarctic continental shelf. *J Geophys Res* 116, C12019.

645 Shi, T., Sun, Y., Falkowski, P.G., 2007. Effects of iron limitation on the expression of
646 metabolic genes in the marine cyanobacterium *Trichodesmium erythraeum* IMS101.
647 *Environmental Microbiology* 9, 2945-2956.

648 Smith, W.O.J., Asper, V.A., Tozzi, S., Liu, X., Stammerjohn, S.E., 2011. Surface
649 layer variability in the Ross Sea, Antarctica as assessed by in situ fluorescence
650 measurements. *Progress in Oceanography* 88, 28-45.

651 Smith, W.O.J., Dennett, M.R., Mathot, S., Caron, D.A., 2003. The temporal dynamics
652 of the flagellated and colonial stages of *Phaeocystis antarctica* in the Ross Sea. *Deep-*
653 *Sea Research II* 50, 605-617.

654 Smith, W.O.J., Dinniman, M.S., Hoffman, E.E., Klinck, J.M., 2014. The effects of
655 changing winds and temperatures on the oceanography of the Ross Sea in the 21st
656 century. *Geophysical Research Letters* 41, 1624-1631.

657 Smith, W.O.J., Dinniman, M.S., Tozzi, S., DiTullio, G.R., Mangoni, O., Modigh, M.,
658 Saggiomo, V., 2010. Phytoplankton photosynthetic pigments in the Ross Sea: Patterns
659 and relationships among functional groups. *Journal of Marine Systems* 82, 177-185.

660 Smith, W.O.J., Dunbar, R.B., 1998. The relationship between new production and
661 vertical flux on the Ross Sea continental shelf. *Journal of Marine Systems* 17, 445-
662 457.

663 Smith, W.O.J., Gordon, L.I., 1997. Hyperproductivity of the Ross Sea (Antarctica)
 664 polynya during austral spring. *Geophysical Research Letters* 24, 233-236.

665 Smith, W.O.J., Jones, R.M., 2015. Vertical mixing, critical depths, and phytoplankton
 666 growth in the Ross Sea. *ICES J Mar Sci* 72, 1952-1960.

667 Smith, W.O.J., Marra, J., Hiscock, M.R., Barber, R.T., 2000. The seasonal cycle of
 668 phytoplankton biomass and primary productivity in the Ross Sea, Antarctica. *Deep-*
 669 *Sea Research II* 47, 3119-3140.

670 Smith, W.O.J., Shields, A.R., Peloquin, J.A., Catalano, G., Tozzi, S., Dinniman, M.S.,
 671 Asper, V.A., 2006. Interannual variations in nutrients, net community production, and
 672 biogeochemical cycles in the Ross Sea. *Deep-Sea Research II* 53, 815-833.

673 Strzepek, R.F., Harrison, P.J., 2004. Photosynthetic architecture differs in coastal and
 674 oceanic diatoms. *Nature* 431, 689-692.

675 Strzepek, R.F., Hunter, K.A., Frew, R.D., Harrison, P.J., Boyd, P.W., 2012. Iron-light
 676 interactions differ in Southern Ocean phytoplankton. *Limnol Oceanogr* 57, 1182-
 677 1200.

678 Strzepek, R.F., Maldonado, M.T., Hunter, K.A., Frew, R.D., Boyd, P.W., 2011.
 679 Adaptive strategies by Southern Ocean phytoplankton to lessen iron limitation:
 680 Uptake of organically complexed iron and reduced cellular iron requirements. *Limnol*
 681 *Oceanogr* 56, 1983-2002.

682 Suggett, D.J., Moore, C.M., Hickman, A.E., Geider, R.J., 2009. Interpretation of fast
 683 repetition rate (FRR) fluorescence: signatures of phytoplankton community structure
 684 versus physiological state. *Mar Ecol Prog Ser* 376, 1-19.

685 Sunda, W.G., Huntsman, S.A., 1997. Interrelated influence of iron, light and cell size
 686 on marine phytoplankton growth. *Nature* 390, 389-392.

687 Tagliabue, A., Arrigo, K.R., 2003. Anomalously low zooplankton abundance in the
 688 Ross Sea: An alternative explanation. *Limnol Oceanogr* 48, 686-699.

689 Tagliabue, A., Arrigo, K.R., 2005. Iron in the Ross Sea: 1. Impact on CO₂ fluxes via
 690 variation in phytoplankton functional group and non-Redfield stoichiometry. *J*
 691 *Geophys Res* 110, C03009.

692 Tagliabue, A., Bopp, L., Aumont, O., 2008. Ocean biogeochemistry exhibits
 693 contrasting responses to a large scale reduction in dust deposition. *Biogeosciences* 5,
 694 11-24.

695 Welschmeyer, N.A., 1994. Fluorometric analysis of chlorophyll-*a* in the presence of
 696 chlorophyll-*b* and pheopigments. *Limnol Oceanogr* 39, 1985-1992.

697 Wu, H., Cockshutt, A.M., McCarthy, A., Campbell, D.A., 2011. Distinctive
698 Photosystem II Photoinactivation and Protein Dynamics in Marine Diatoms. *Plant*
699 *Physiology* 156, 2184-2195.
700

Tables and Figure Legends

Table 1 Locations for long-term experiments conducted during NBP12-01 along with values of initial F_v/F_m , $\Delta(F_v/F_m)$ (Equation 1), net growth rates estimated from chlorophyll accumulation (Supplementary Information, Equation S1) and nitrate drawdown (Supplementary Information, Equation S2) over 168 h. Shown are averages \pm standard errors ($n = 3$ or 5), * indicate significant differences (Two-way ANOVA, $p < 0.05$) from control.

Figure 1 Composite map of Southern Ocean MODIS chlorophyll a for December 2011 – February 2012. Inset: Long-term (blue dots) and short-term (red dots) experimental locations conducted on cruise NBP12-01 in the Ross Sea with 250 m bathymetric contours. Surface *in situ* samples were also collected at these locations and at those marked CTD-station (black dots).

Figure 2 Surface chlorophyll concentrations ($\mu\text{g L}^{-1}$) from CTD stations (a). Surface DIN concentrations (μM) (b). Surface F_v/F_m (c). Surface DFe concentrations (nM) (d). Chlorophyll, DIN and F_v/F_m from samples collected at 1-5 m depth, DFe from samples collected at ~ 10 m depth.

Figure 3 Matrix of Pearson's linear correlation coefficients between the variables measured in the surface waters of the Ross Sea, including: sea surface temperature (SST), Nitrate (DIN), Phosphate (PO_4^{3-}), Silicate (Si), community structure (% Diatoms), chlorophyll concentration, F_v/F_m , σ_{PSII} , $F_m:\text{PsbA}$, $\text{Chl}:\text{PsbA}$, and dissolved iron concentrations (DFe). The strength of the linear association between each pair of variables is indicated by the colour of the square, with the negative and positive correlations denoted by '-' and '+' within all squares where significant ($p < 0.01$).

Figure 4 Spatial distribution of $\Delta(F_v/F_m)$ calculated from Fe addition incubation experiments (a). $\Delta(F_v/F_m)$ calculated from long-term Fe-addition incubation experiments in the Ross Sea, both from (1) near the Ross Ice Shelf, (2) over the Ross Bank and (3) within an anti-cyclonic eddy (b). The change in chlorophyll normalized maximum fluorescence, ($\Delta F_m \text{ Chl}^{-1}$) from the three long-term Fe addition incubation experiments (c). The change in chlorophyll normalized variable fluorescence $\Delta(F_v \text{ Chl}^{-1})$ from the three long-term Fe addition incubation

experiments **(d)**. Shown are averages with \pm standard errors ($n = 4$ or 5). * represent statistically significant differences (*t-test*, $p < 0.05$).

Figure 5 Relationship of DIN (μM) and photosynthetic efficiency (F_v/F_m) throughout the Ross Sea as a function of a) chlorophyll concentrations ($\mu\text{g L}^{-1}$), b) phytoplankton composition (%), and c) the relative degree of Fe stress $\Delta(F_v/F_m)$ **(c)**. Grey dots represent stations where DIN and F_v/F_m were measured but no corresponding additional variables were measured.

Figure 6 Relationship of DIN (μM) and photosynthetic efficiency (F_v/F_m) throughout the Ross Sea as a function of a) functional cross-section of photosystem II (σ_{PSII}) (nm^{-2}), b) the ratio of chlorophyll to PsbA (a core subunit of PSII) (mmol mol^{-1}), c) the ratio of the maximum fluorescence yield to chlorophyll ($F_m:\text{Chl}$), and d) the ratio of the maximum fluorescence yield to PsbA ($F_m:\text{PsbA}$). Grey dots represent stations where DIN and F_v/F_m were measured but no corresponding additional variables were measured.

Table 1

Experiment	1	2	3
Lat (°S)	75.72	76.72	77.55
Long (°W)	183.40	179.08	175.97
F_v/F_m Initial	0.26 ±0.01	0.29 ±0.00	0.21 ±0.00
Δ (F_v/F_m), 24 h	0.04 ±0.01	0.00 ±0.00	0.01 ±0.00
μ^{chl}_{Control} (d⁻¹), 0 -168 h	0.11 ±0.02	0.25 ±0.01	0.13 ±0.01
μ^{chl}_{Fe} (d⁻¹), 0 -168 h	0.17* ±0.02	0.29* ±0.00	0.19* ±0.01
ΔNO₃⁻ Control (μ M d⁻¹), 0 – 168 h	1.61 ±0.33	1.50 ±0.04	2.43 ±0.08
ΔNO₃⁻ Fe (μ M d⁻¹), 0 – 168 h	2.53* ±0.13	1.57 ±0.05	2.93* ±0.07

Figure 1

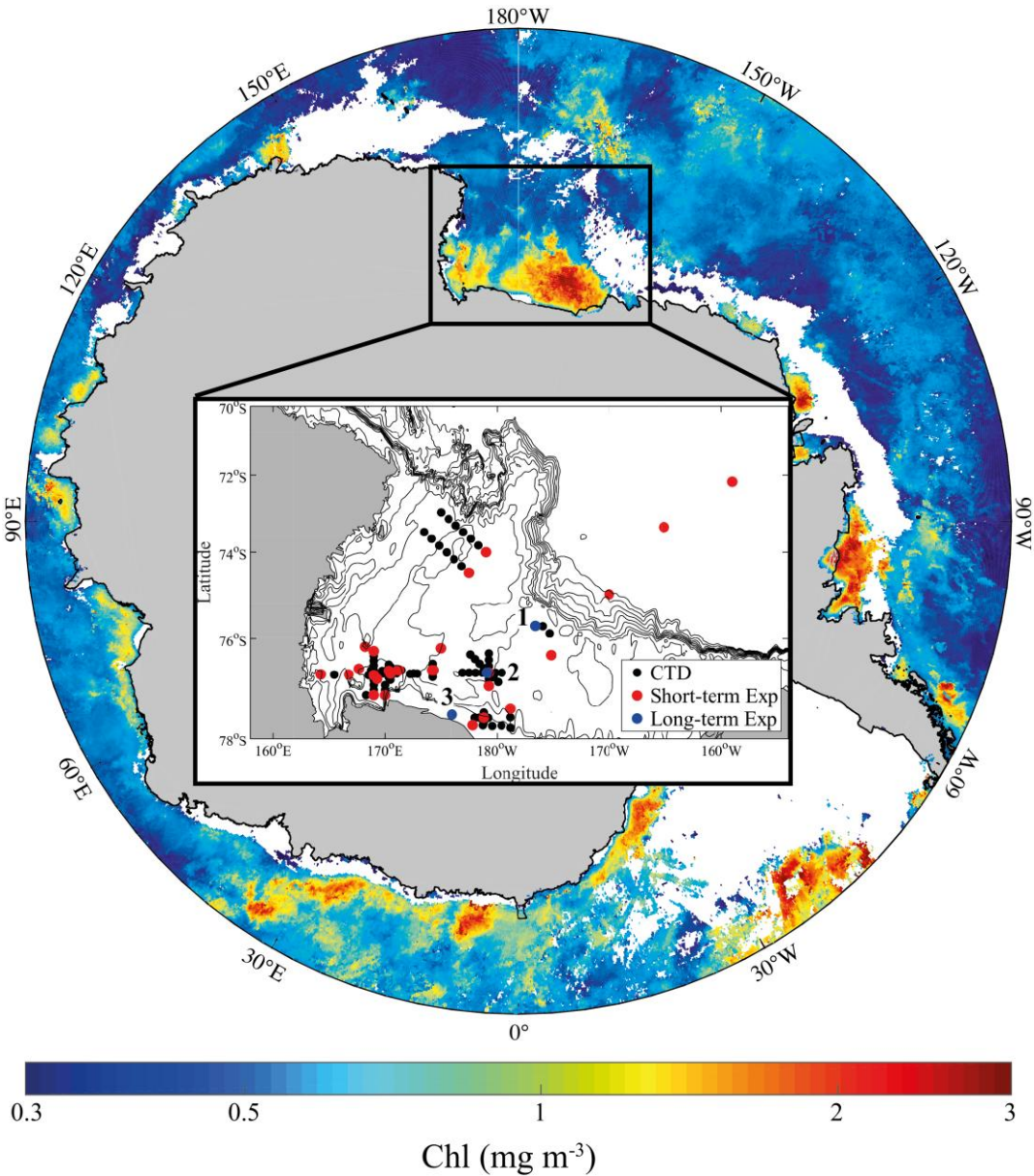
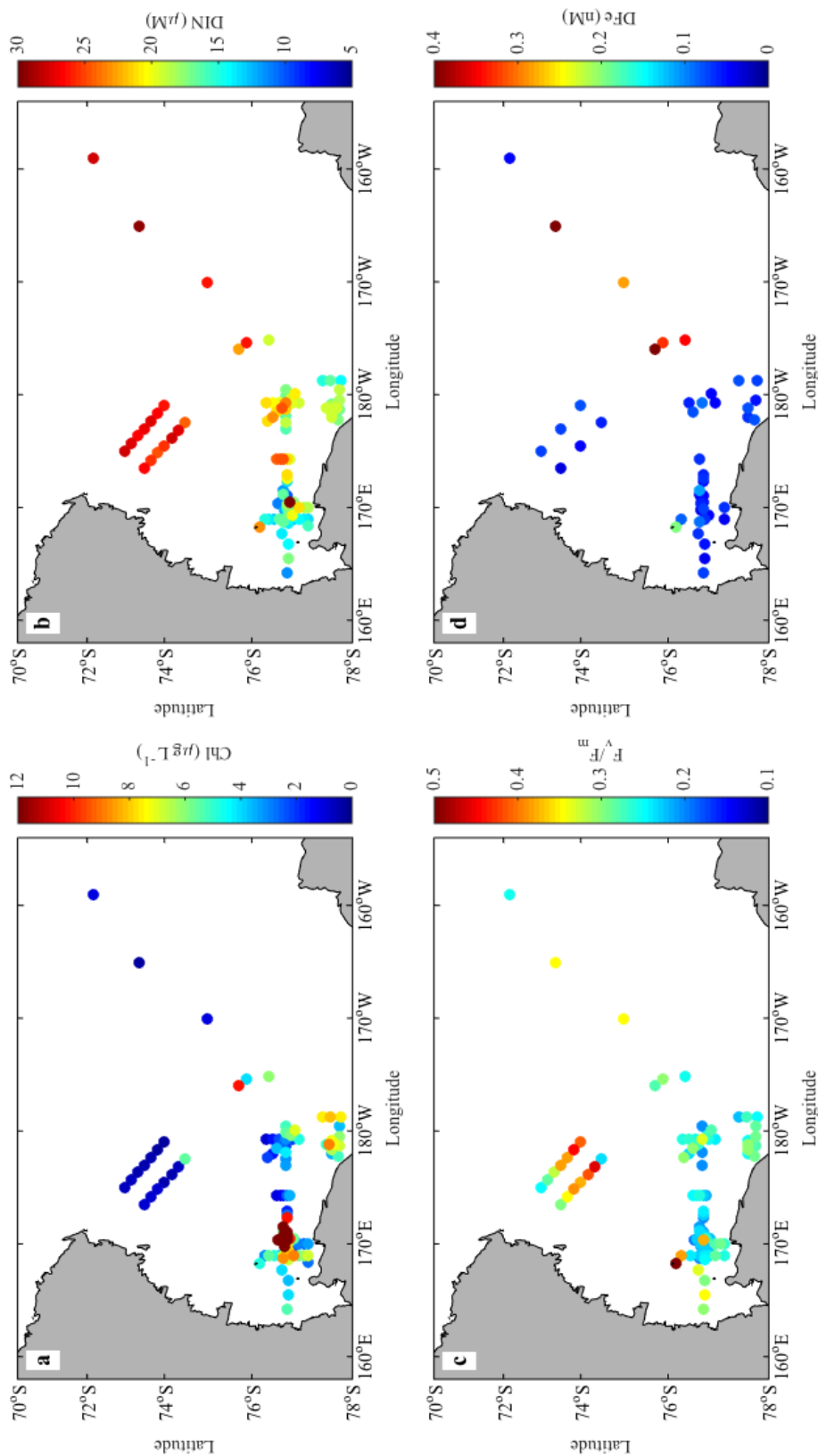
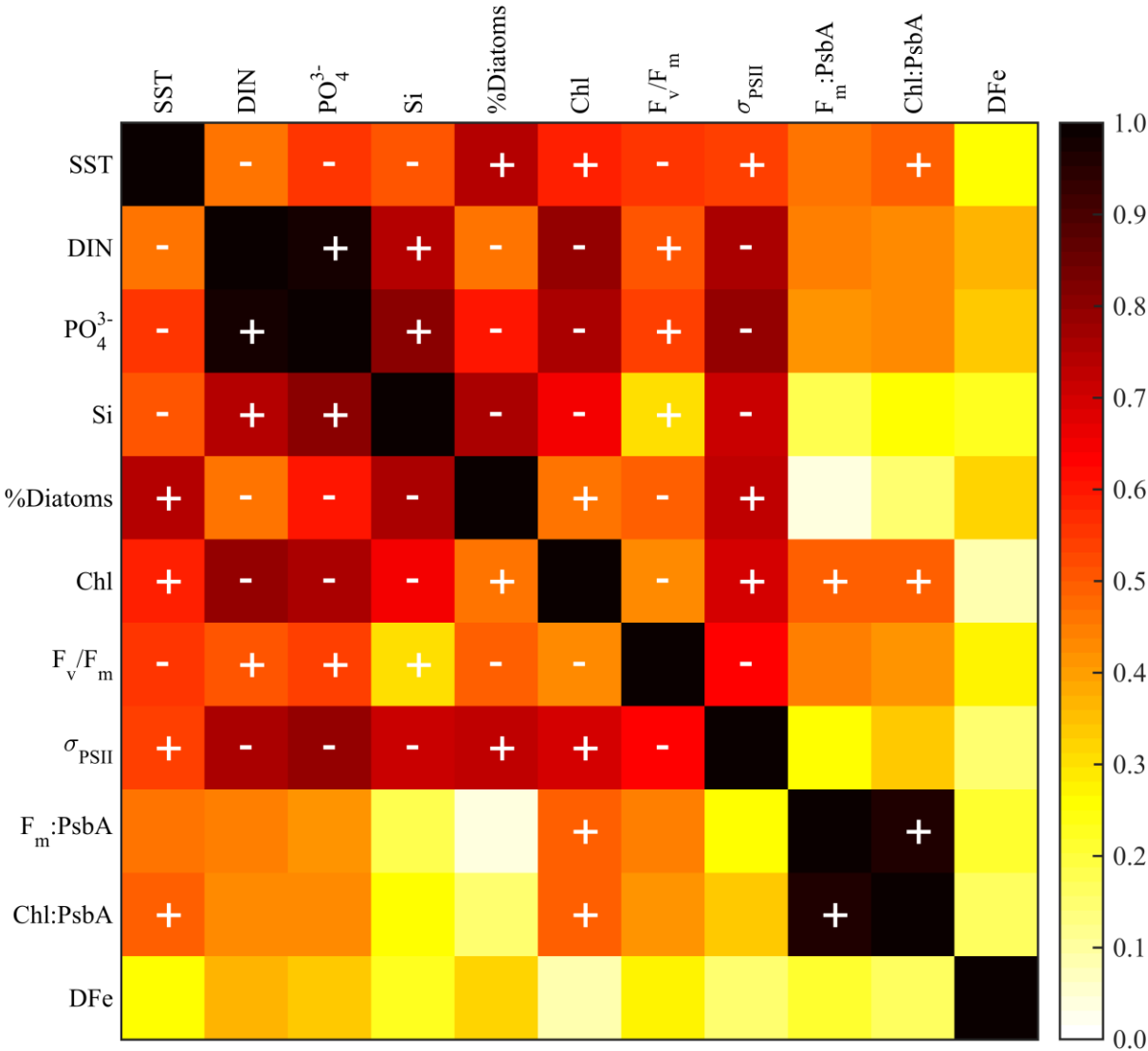


Figure 2



759 Figure 3



760

761

Figure 4

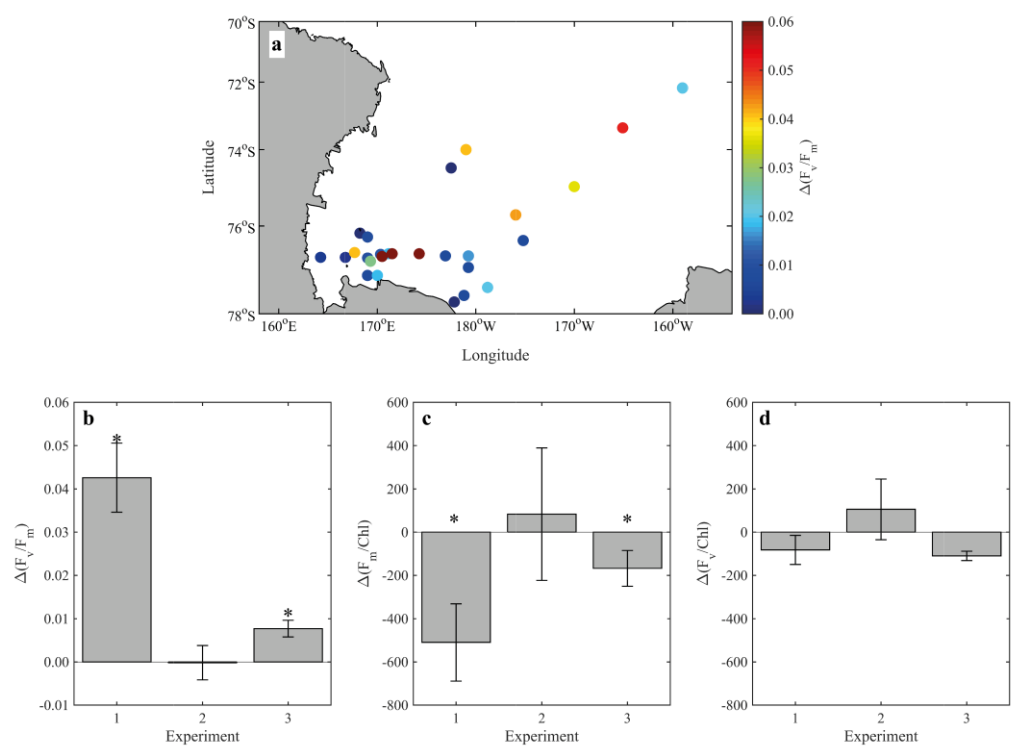


Figure 5

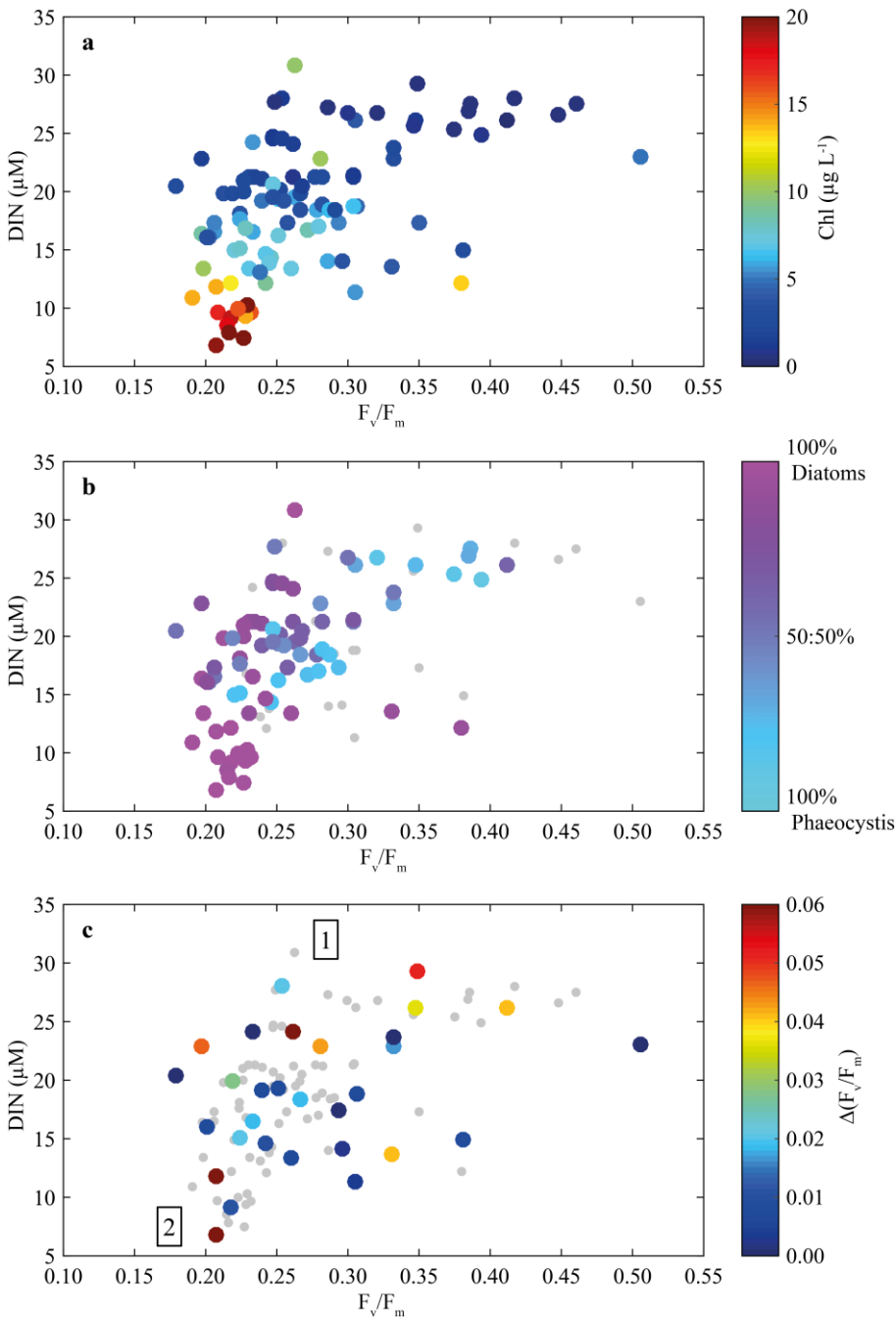


Figure 6

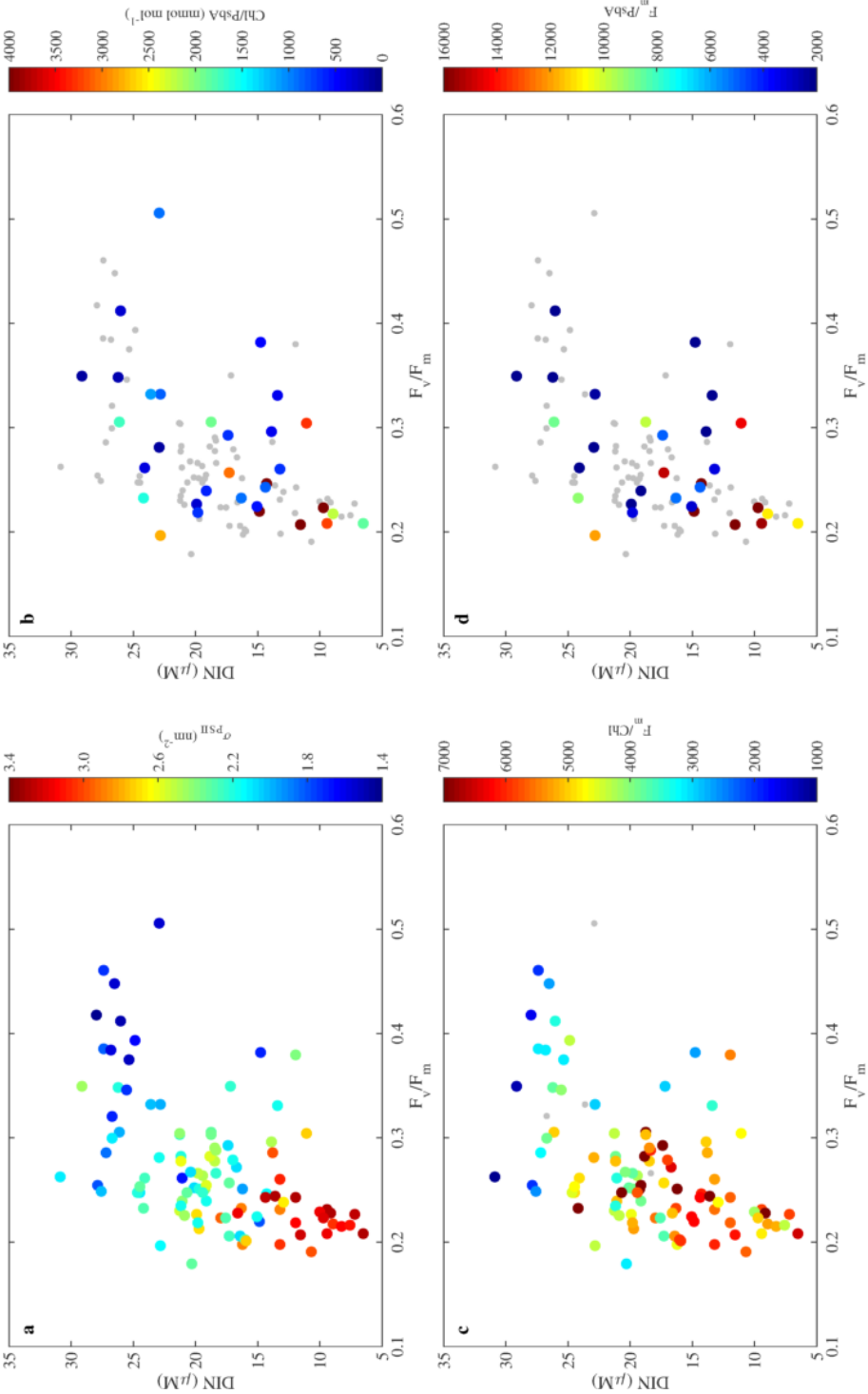


Figure 1
[Click here to download Figure\(s\): prism_fig1.eps](#)

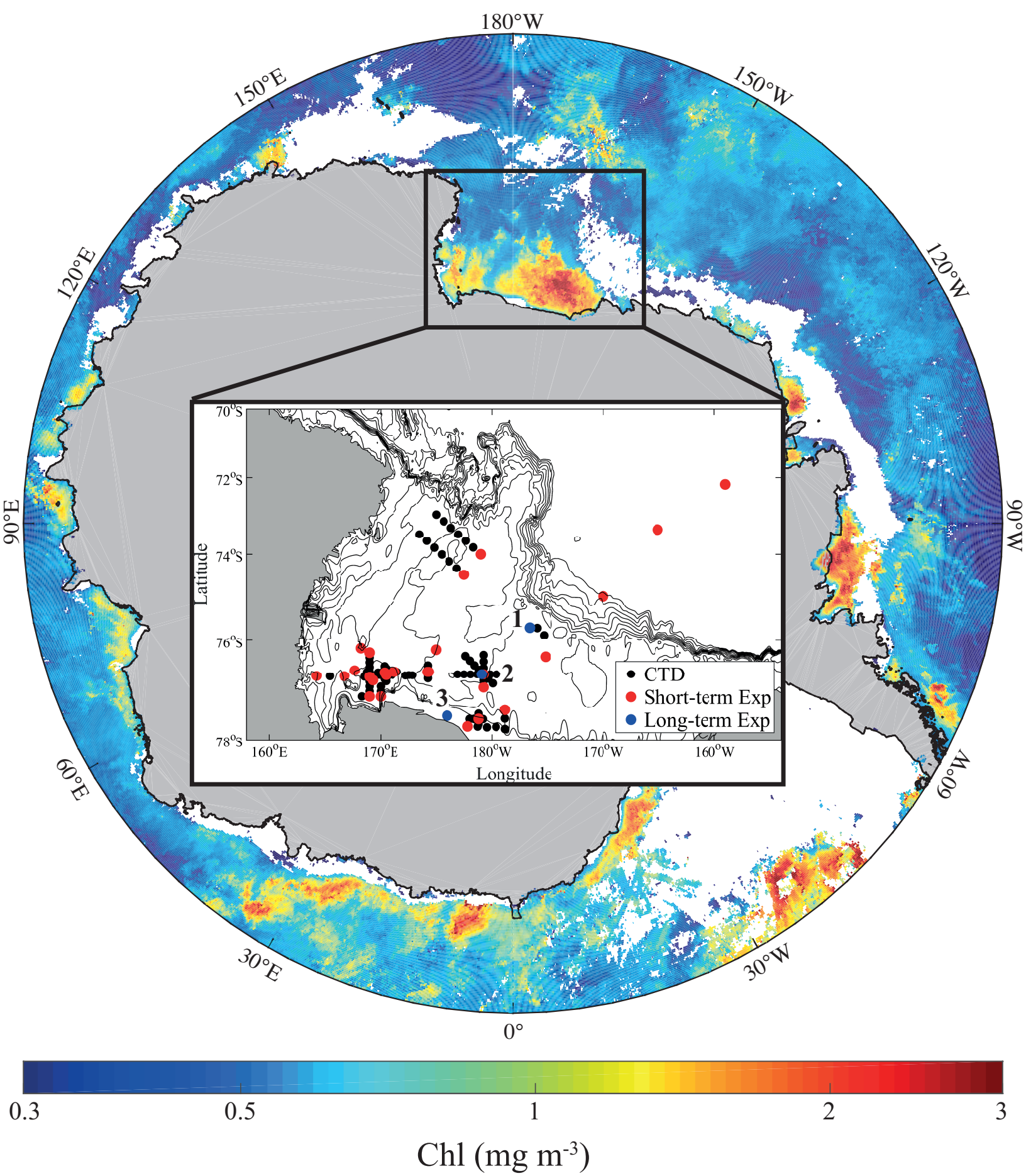


Figure 2
[Click here to download Figure\(s\): prism_fig2.eps](#)

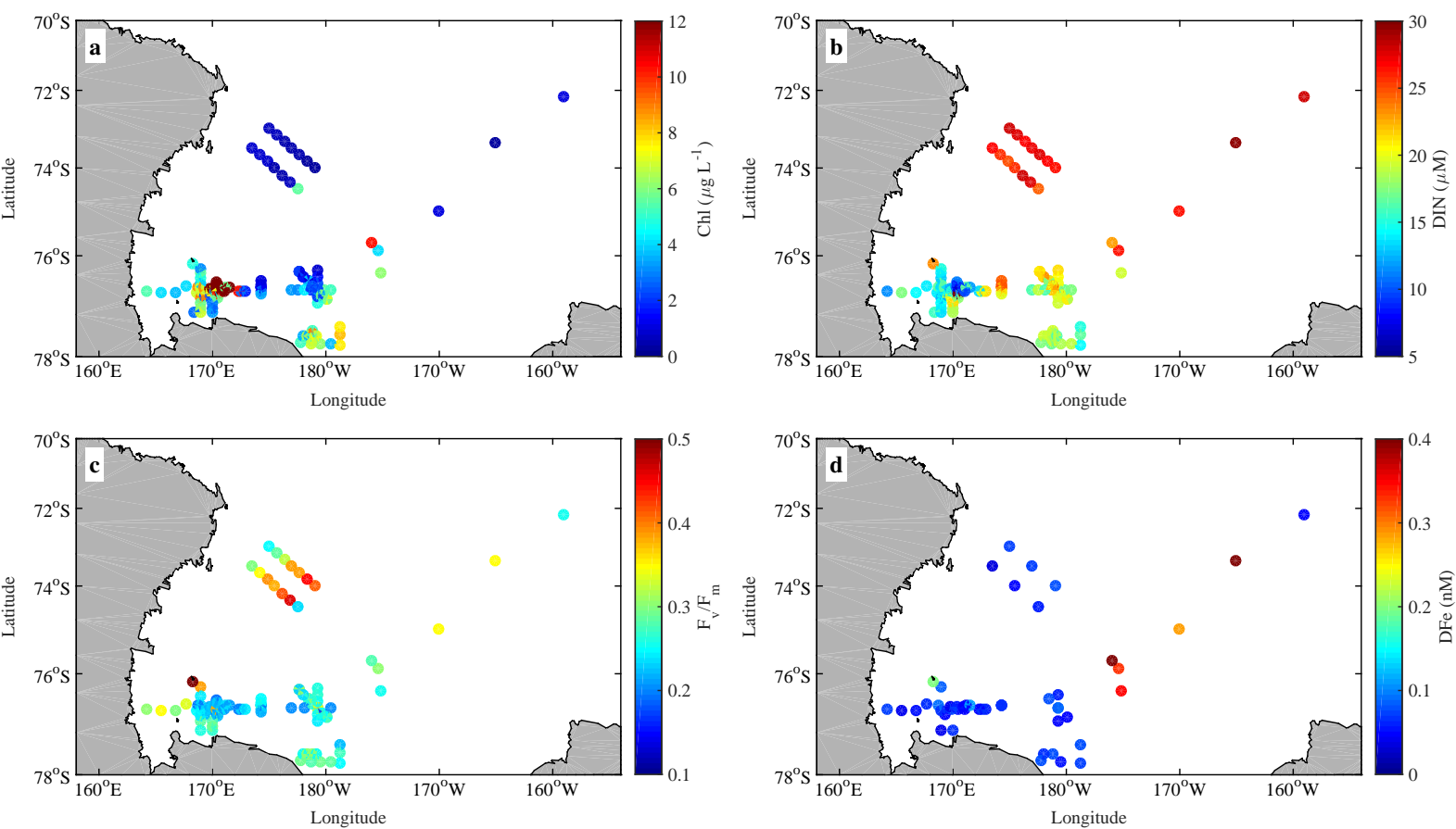


Figure 3
[Click here to download high resolution image](#)

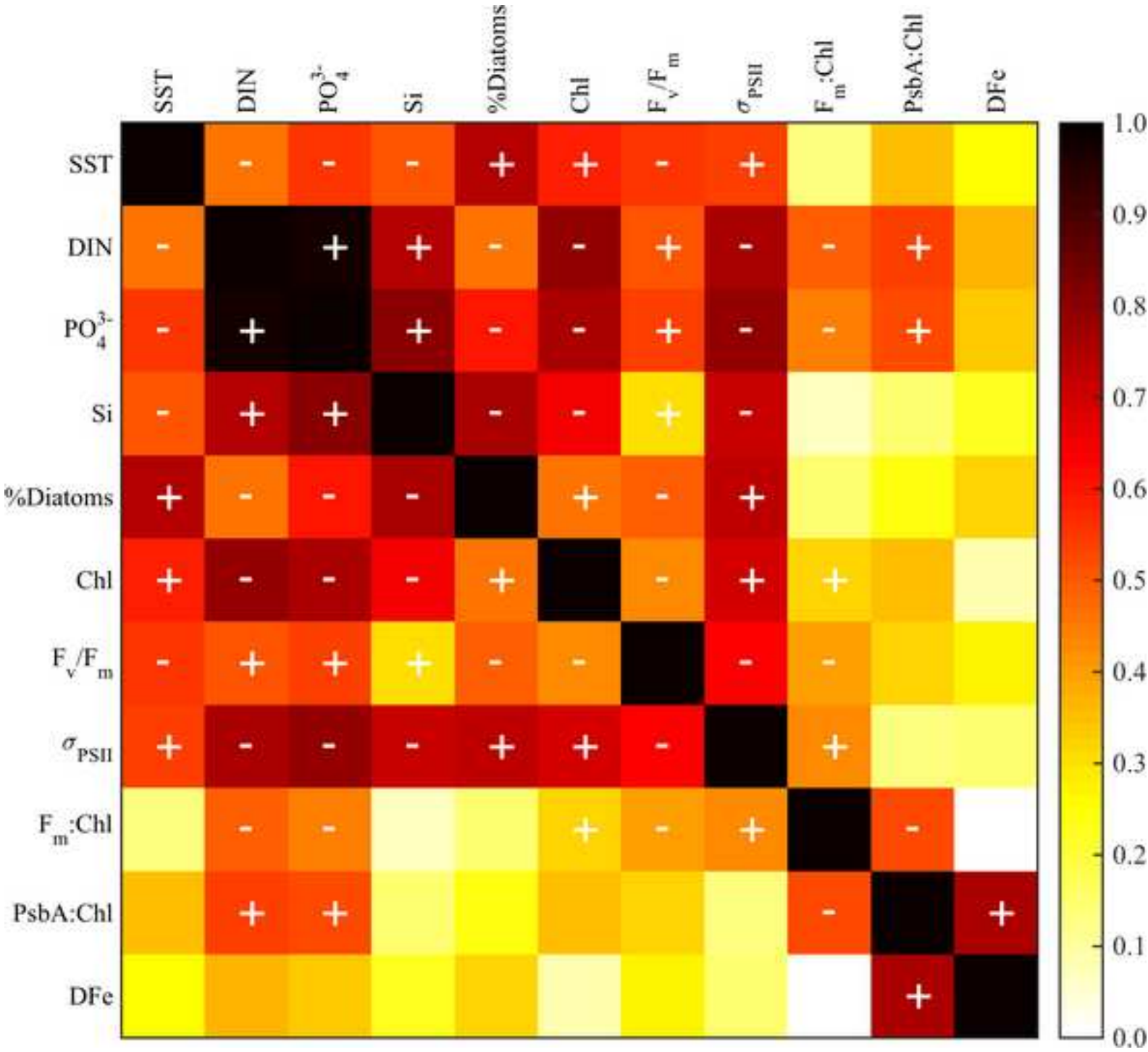
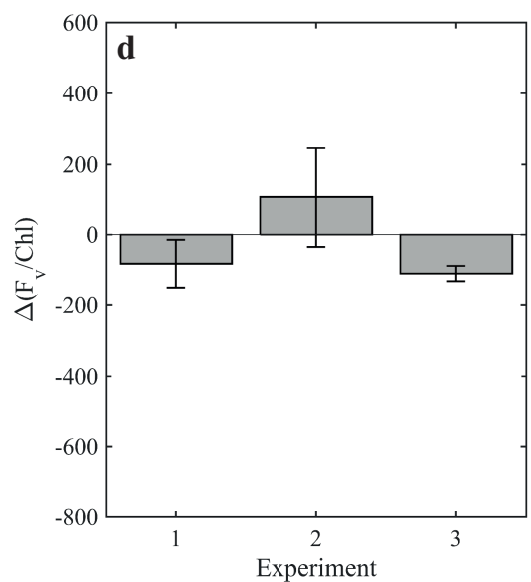
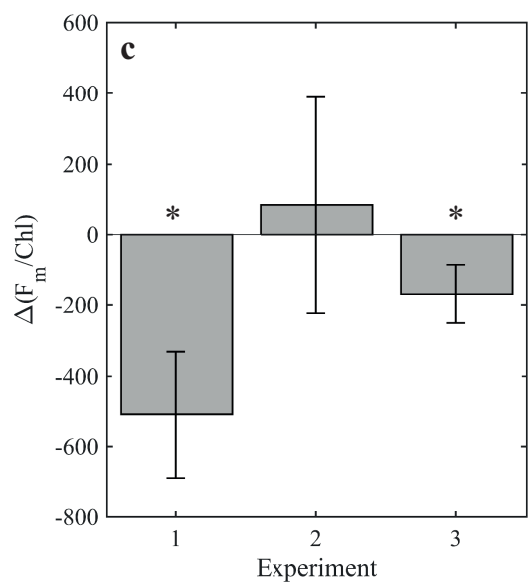
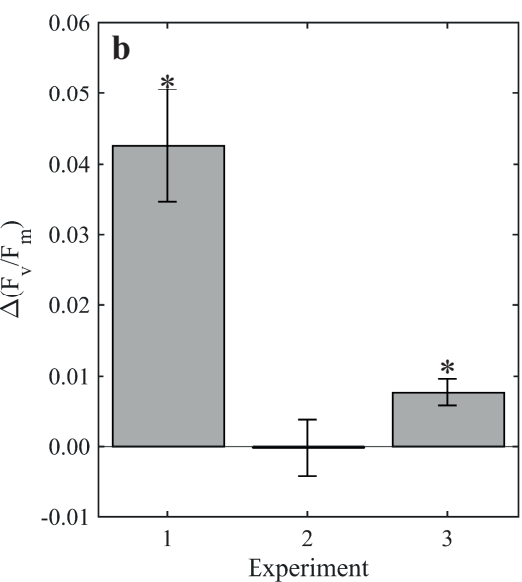
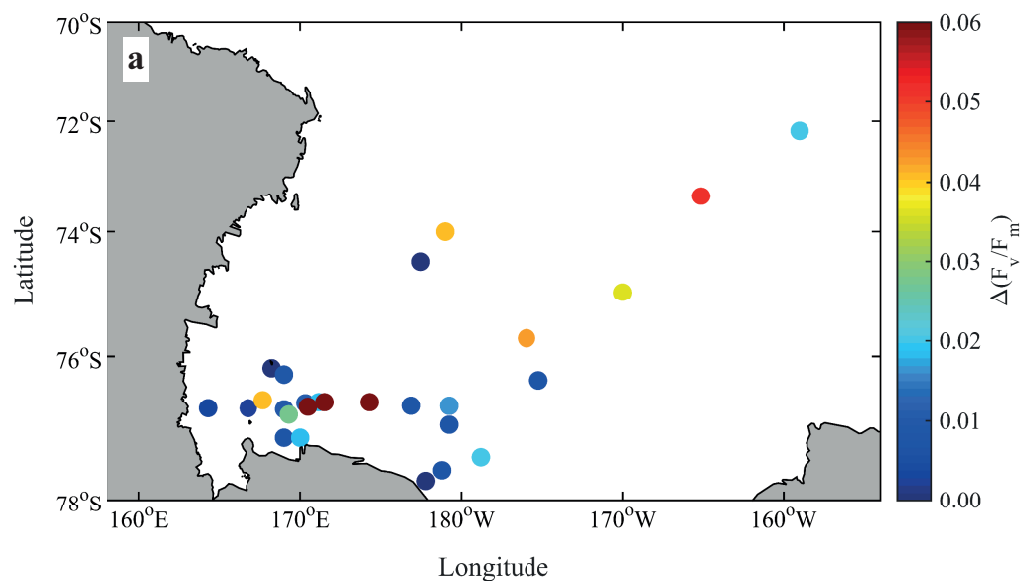


Figure 4
[Click here to download Figure\(s\): prism_fig4.eps](#)



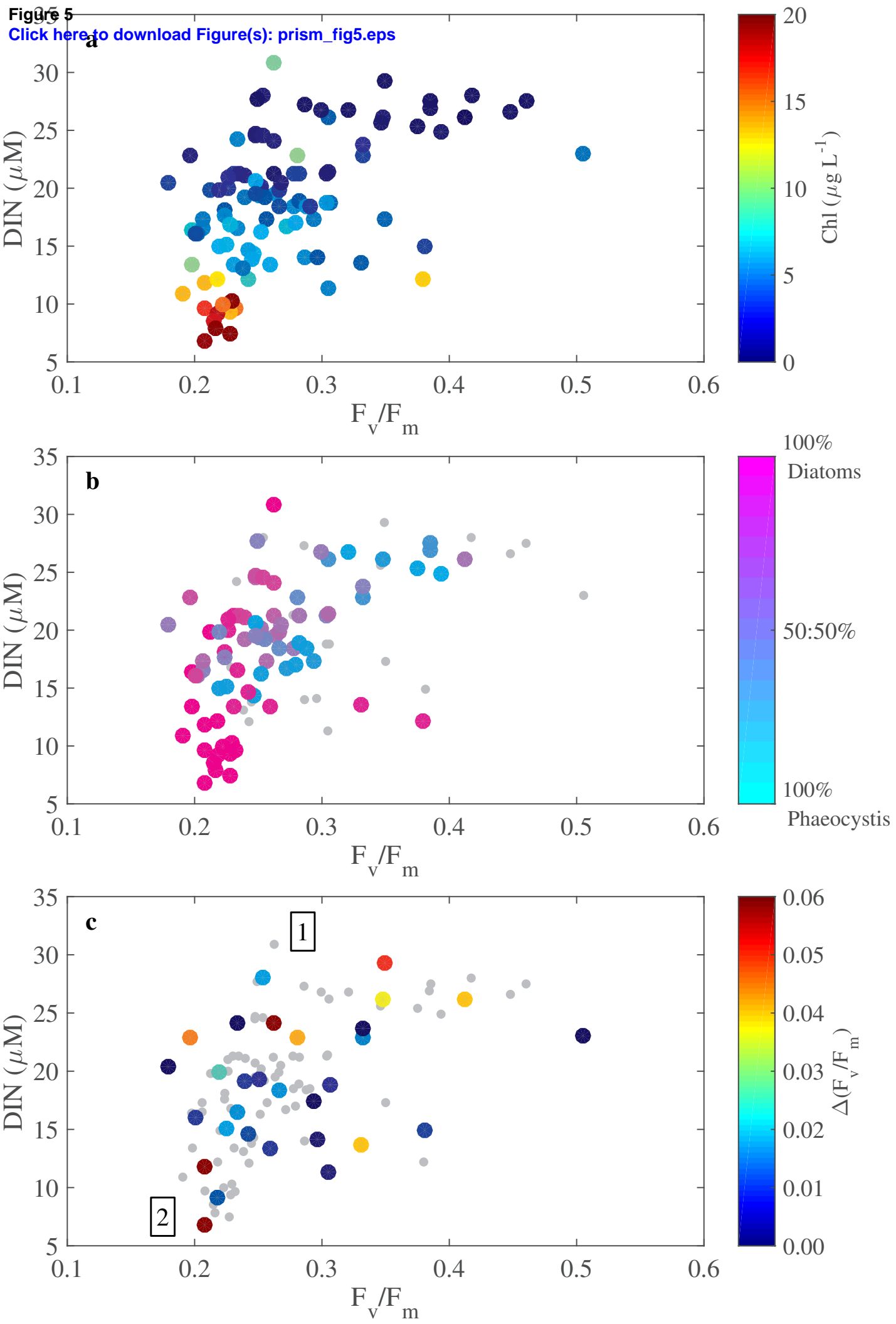


Figure 6
[Click here to download Figure\(s\): prism_fig6.eps](#)

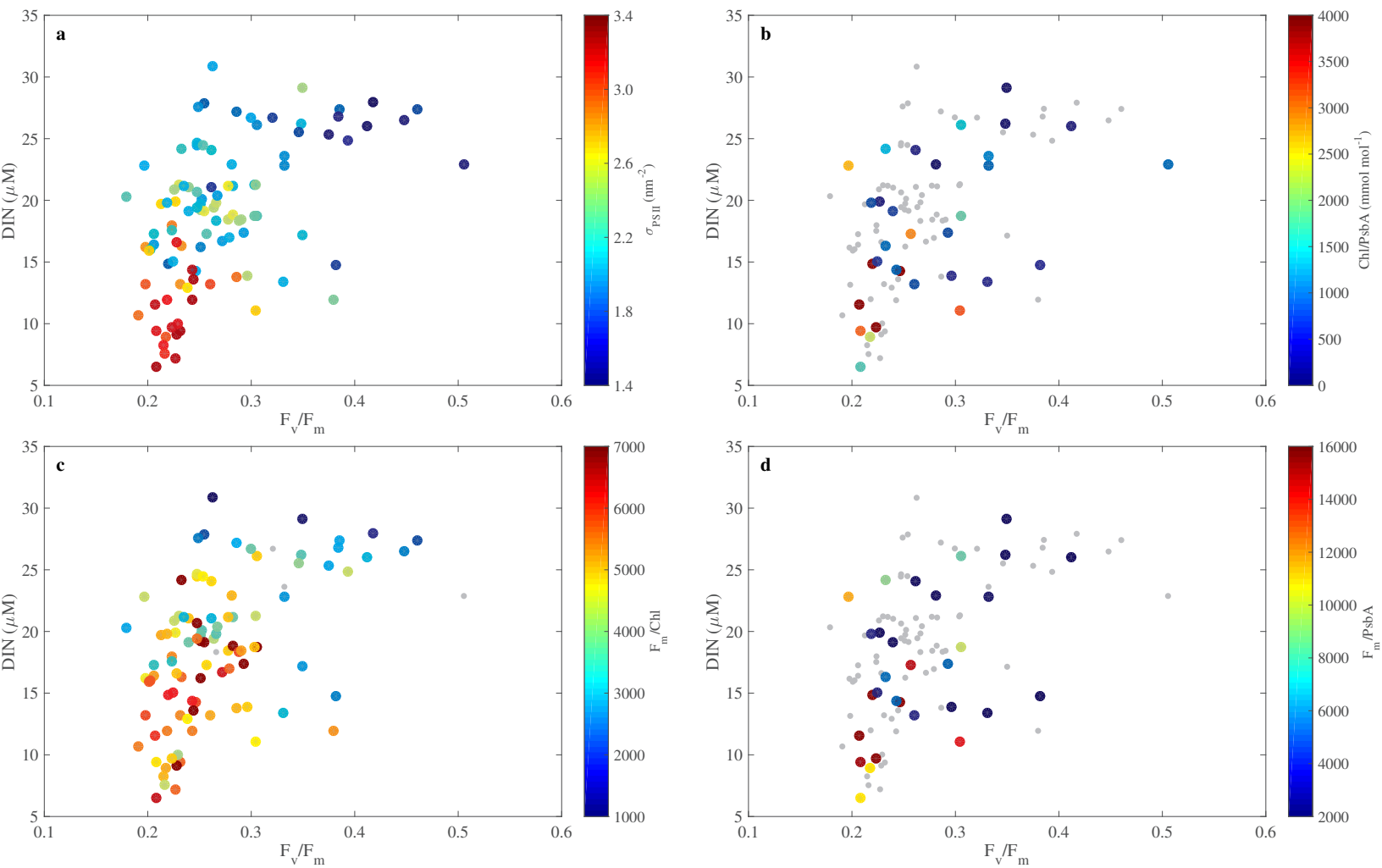


Figure S1
[Click here to download high resolution image](#)

